Author Manuscript

Author Manuscript

Author Manuscript

Author Manuscript

HHS Public Access

Author manuscript

Nature. Author manuscript; available in PMC 2015 May 13.

Published in final edited form as:

Nature. 2014 November 13; 515(7526): 264–268. doi:10.1038/nature13973.

Radial glia require PDGFD/PDGFRß signaling in human but not mouse neocortex

Jan H. Lui[1,2,4], **Tomasz J. Nowakowski**[1,2,4], **Alex A. Pollen**[1,2], **Ashkan Javaherian**[1,2,3], **Arnold R. Kriegstein**[1,2], and **Michael C. Oldham**[1,2]

Arnold R. Kriegstein: kriegsteina@stemcell.ucsf.edu; Michael C. Oldham: oldhamm@stemcell.ucsf.edu

[1]Department of Neurology

[2]Eli and Edythe Broad Center of Regeneration Medicine and Stem Cell Research, University of California, San Francisco, 35 Medical Center Way, San Francisco, CA 94143

Abstract

Evolutionary expansion of the human neocortex underlies many of our unique mental abilities. This expansion has been attributed to the increased proliferative potential[1, 2] of radial glia (RG; i.e. neural stem cells) and their subventricular dispersion from the periventricular niche[3, 4, 5] during neocortical development. Such adaptations may have evolved through gene expression changes in RG. However, whether or how RG gene expression varies between humans and other species is unknown. Here we show that the transcriptional profiles of human and mouse neocortical RG are broadly conserved during neurogenesis, yet diverge for specific signaling pathways. By analyzing differential gene coexpression relationships between the species, we demonstrate that the growth factor *PDGFD* is specifically expressed by RG in human, but not mouse, corticogenesis. We further show that the expression domain of PDGFRß, the cognate receptor[6, 7] for PDGFD, is evolutionarily divergent, with high expression in the germinal region of dorsal human neocortex but not in the mouse. Pharmacological inhibition of PDGFD/PDGFRß signaling in slice culture prevents normal cell cycle progression of neocortical RG in human, but not mouse. Conversely, injection of recombinant-PDGFD or ectopic expression of constitutively active PDGFRß in developing mouse neocortex increases the proportion of RG and their subventricular dispersion. These findings highlight the requirement of PDGFD/PDGFRß signaling

Users may view, print, copy, and download text and data-mine the content in such documents, for the purposes of academic research, subject always to the full Conditions of use:http://www.nature.com/authors/editorial_policies/license.html#terms

Correspondence to: Arnold R. Kriegstein, kriegsteina@stemcell.ucsf.edu; Michael C. Oldham, oldhamm@stemcell.ucsf.edu.

[3]Present address: Gladstone Institute of Neurological Disease, 1650 Owens St, San Francisco, CA 94158

[4]These authors contributed equally

Reprints and permissions information is available at www.nature.com/reprints.

The authors declare no conflict of interests.

AUTHOR CONTRIBUTIONS: M.C.O. conceived the GCASS strategy and J.H.L generated the GCASS dataset. A.J. generated the FACS-mRG dataset. M.C.O. conceived, designed, and performed the bioinformatic analyses. J.H.L., T.J.N., and A.A.P. designed and performed the experiments leading up to the prioritization of PDGFD as the focus of this study. T.J.N. performed the majority of the *in situ* hybridizations and the *in vivo* mouse experiments. J.H.L. performed the human and mouse slice culture experiments, as well as all of the immunostaining, imaging, and image analysis in the study. M.C.O. and J.H.L. wrote the manuscript, which was edited by all the authors. M.C.O. and A.R.K provided conceptual guidance at every stage of the project.

Statements: Microarray data from the GCASS dataset have been deposited in Gene Expression Omnibus (http://www.ncbi.nlm.nih.gov/geo/) under accession ID GSE62064.

Author Manuscript Author Manuscript Author Manuscript Author Manuscript

for human neocortical development and suggest that local production of growth factors by RG supports the expanded germinal region and progenitor heterogeneity of species with large brains.

RG are the physical substrate[8] and progenitor population that underlie production of most cells in human neocortex[2]. We sought to determine a general transcriptional "signature" of human neocortical RG (hRG) as a starting point for identifying genes that may regulate uniquely human aspects of cortical development. We and others have previously shown that gene coexpression analysis of heterogeneous tissue samples can deconvolve transcriptional signatures of distinct cell types without cell isolation or purification[9, 10]. Because prenatal samples of human neocortex are scarce, we developed a novel strategy called **G**ene **C**oexpression **A**nalysis of **S**erial **S**ections (**GCASS**) that exploits variation in cellular abundance across serial sections of a single tissue sample to reveal cell type-specific patterns of gene expression (Fig. 1a-c; Extended Data Fig. 1; see Supplementary Information for methods, rationale, and further discussion). We applied GCASS to 87 150μm sections of a single human cortical sample from gestational week 14.5 (GW14.5, corresponding to peak layer V neurogenesis[11]; Supplementary Table 1) and identified 55 modules of coexpressed genes. Six modules overlapped significantly with a set of genes we determined were expressed significantly higher in FACS-sorted mouse RG (mRG) vs. intermediate progenitor cells ("FACS-mRG": Extended Data Fig. 1; Supplementary Table 2), suggesting that they might represent transcriptional signatures of hRG (Fig. 1d). Analysis of laser-microdissected samples from three independent transcriptomic datasets[12, 13] confirmed that genes in these modules are most highly expressed in the ventricular zone (VZ) and subventricular zone (SVZ) of developing human neocortex, where both ventricular (vRG) and outer subventricular (oRG) subtypes of RG reside[4] (Extended Data Fig. 2).

To produce a consensus transcriptional signature for GW14.5 hRG, we first summarized each of these six modules by its first principal component/module eigengene[14, 15] (ME) and calculated the WGCNA[16] measure of intramodular gene connectivity, kME[10, 14] (concept: Fig. 1c). kME quantifies the extent to which a gene conforms to the characteristic expression pattern of a module and can predict gene expression specificity for individual cell types[10]. kME values for the six modules were combined into a single measure (*Z.hRG*), with higher scores predicting greater expression specificity for hRG (Fig. 1e). Genes with high *Z.hRG* included markers of neocortical RG such as *SLC1A3* (*GLAST1*), *VIM*, *SOX2*, *NOTCH1*, and *PAX6* (Fig. 1e: blue lines). Genes with low *Z.hRG* included markers of committed neuronal lineages such as *TBR1*, *FEZF2*, *RELN*, and *SATB2* (Fig. 1e: black lines). We performed *in situ* hybridization (ISH) and immunostaining on independent prenatal human neocortical samples for genes with high *Z.hRG* that have not, to the best of our knowledge, previously been implicated in RG biology (Fig. 1e: red lines; Extended Data Fig. 3). In all cases, expression of these genes was restricted to the VZ/SVZ (Fig. 1f; Extended Data Fig. 3). These results indicate that GCASS can discern a general transcriptional signature of hRG from a single, heterogeneous tissue sample without cell labeling, isolation, or purification. Moreover, because the sample derives from a single individual, this strategy implicitly controls for genotype and developmental stage and has broad implications for the molecular analysis of rare tissue samples.

Author Manuscript Author Manuscript Author Manuscript Author Manuscript

To establish the robustness of the hRG transcriptional signature, we analyzed four additional prenatal human cortex gene expression datasets[12, 13, 17] that were generated with diverse sampling strategies and technology platforms (Extended Data Table 1). In parallel, we also analyzed three embryonic mouse cortex gene expression datasets[12, 18, 19] (largely E14-14.5, corresponding to peak layer V neurogenesis[11]; Extended Data Table 1) to establish a robust mRG transcriptional signature. For each dataset, we constructed an unsupervised coexpression network, identified the module with the most significant overlap with the FACS-mRG gene set, and calculated kME values (RG.kME) for every gene with respect to this RG module (Supplementary Table 3). To facilitate comparisons of RG transcriptional signatures, we mapped all probe sets/transcripts to a common identifier (HomoloGene ID) and converted RG.kME values for each dataset into percentile ranks (RG.PR; workflow schematic: Extended Data Fig. 4). Genome-wide correlations of RG.PR among all datasets ranged from 0.36 – 0.95 (human) and 0.47 – 0.70 (mouse) ($P < 2.2e-16$; Extended Data Fig. 5), demonstrating the robustness of RG transcriptional signatures in both species.

To explore the global extent of gene expression conservation between hRG and mRG, we calculated the mean RG specificity for each gene across the five human ($\overline{\mathrm{hRG.PR}}$), three mouse ($\overline{\mathrm{mRG.PR}}$), and all eight ($\overline{\mathrm{RG.PR}}$) datasets (Supplementary Table 3). For genes present in at least one dataset in each species (n = 15,576), the correlation between $\overline{\mathrm{hRG.PR}}$ and $\overline{\mathrm{mRG.PR}}$ was 0.48 ($P < 2.2e-16$; Fig. 2a), indicating broad conservation of transcriptional programs that are active during cortical development in humans and mice. Genes with $\overline{\mathrm{hRG.PR}}$ and $\overline{\mathrm{mRG.PR}} > 80$ (Fig. 2a, +RG box) or < 20 (Fig. 2a, -RG box) were significantly enriched with sets of genes expressed by RG or neurons, respectively (Supplementary Table 4). Furthermore, the most conserved set of core RG genes ($\overline{\mathrm{hRG.PR}}$ and $\overline{\mathrm{mRG.PR}} > 95$: Fig. 2a, green box) included the canonical RG markers *VIM* and *PAX6*, and *SOX* family members implicated in nervous system development such as *Sox2*, *SOX3*, *SOX9*, and *SOX21* (Fig. 2b). Also present among this core set were elements of the Notch (*NOTCH2* and *HES1*) and Wnt-βcatenin (*SFRP1*, *FZD8*, and *LRP4*) signaling pathways, which critically regulate neurogenesis[2]. In addition, we observed a cohesive subgroup of genes involved in cell cycle regulation, including *CKS2*, *RACGAP1*, *MELK*, *CCNB1*, *CCNA2*, *ASPM*, and *MKI67*. Finally, several genes in this group have not, to the best of our knowledge, previously been implicated in RG biology, including *PSAT1*, *DDAH1*, *AIF1L*, *PSRC1*, and *ACSS1*. Together, these results provide a framework for identifying conserved and distinct aspects of gene expression in hRG and mRG.

To identify evolutionary changes in RG gene expression that might underlie neurodevelopmental differences between human and mouse, we assessed homologous genes based on predicted differences in RG expression specificity between the species (differential RG specificity: $\mathrm{DS} = \overline{\mathrm{hRG.PR}} - \overline{\mathrm{mRG.PR}}$). Because such differences could emerge from gene expression changes in RG or neighboring cell types (Fig. 2c), we also compared the relative expression levels of homologous genes between the species (differential expression: $\mathrm{DE} = \overline{\mathrm{h.Expr.PR}} - \overline{\mathrm{m.Expr.PR}}$). Genome-wide analysis of DS/DE revealed four distinct quadrants of genes that differed substantially between human and mouse (Fig. 2d). Consistent with the proposed model (Fig. 2c), these quadrants were enriched with sets of

Author Manuscript Author Manuscript Author Manuscript Author Manuscript

genes expressed in distinct patterns in developing human and mouse cortex (Supplementary Table 4).

We reasoned that quadrant 1 might contain genes with "Boolean" expression differences (i.e. ON in hRG and OFF in mRG) required for human but not mouse neocortical development. We applied stringent criteria to identify and validate 18 candidate genes in this quadrant with strong and consistent evidence of expression in hRG and no evidence of expression in mRG: *ABHD3*, *ASAP3*, *BMP7*, *C5*, *C8orf4*, *FAM107A*, *FOXN4*, *ITGA2*, *LRIG3*, *LRRC17*, *PAM*, *PDGFD*, *PDLIM3*, *RFTN2*, *SLC2A10*, *SP110*, *STOX1*, and *ZC3HAV1* (Fig. 2d, cyan circles; Extended Data Fig. 6). Because secreted growth factors could alter the size of developing neocortex by influencing proliferation, we focused on *PDGFD* (Fig. 2d', green square), which has not, to the best our knowledge, previously been implicated in cortical development of any species. Compared to genes with the highest $\overline{\mathrm{RG.PR}}$ (conserved in both species), *PDGFD* expression was highly correlated in human, but not mouse (Fig. 3a-b). ISH confirmed that *PDGFD* was expressed by RG throughout the VZ of GW14.5 human neocortex (Fig. 3c). In contrast, *Pdgfd* was not detected in RG (or any cell type) in E15.5 mouse neocortex (Fig. 3d). These expression differences were consistent for multiple ages in human (GW14.5-GW18.2) and mouse (E14.5-E17.5) prenatal cortex (Extended Data Fig. 7).

The effects of PDGFD are specifically mediated by the PDGFRß receptor, which upon phosphorylation can trigger signaling pathways that promote cell proliferation[6, 7, 20]. Although *PDGFRβ* did not meet the same stringent criteria as *PDGFD*, its location on the DS/DE plot was proximal to *PDGFD* (Fig. 2d', red square), also suggesting species differences in *PDGFRβ* expression. Compared to genes with the highest $\overline{\mathrm{RG.PR}}$, *PDGFRβ* expression was moderately correlated in human, but not mouse (Fig. 3e-f). Immunostaining for PDGFRß in GW14.5 human brain revealed strong expression throughout the telencephalic germinal zones (VZ/SVZ) and in vascular pericytes, with highest levels in dorsolateral cortical progenitors and the lateral ganglionic eminence (LGE) (Fig. 3g). In contrast, immunostaining for PDGFRß in E15.5 mouse brain revealed expression in LGE progenitors but no evidence of expression in cortical progenitors (Fig. 3h). However, we did observe very low levels of *Pdgfrβ* transcript in the VZ of lateral mouse cortex[21] (Extended Data Fig. 8), leaving open the possibility of modest, region-specific function. Collectively, these results indicate that expression patterns of PDGFD and PDGFRß in developing neocortex have diverged considerably during human and mouse evolution, despite retaining amino-acid sequences that are ∼85% identical between the species.

We tested the requirement of PDGFD/PDGFRß signaling for hRG proliferation in GW17.5 human neocortical slice cultures, screening four chemical inhibitors of PDGFRß signaling (Sutent, Tivozanib, Imatinib, and CP673451). Three out of four PDGFRß inhibitors reduced the percentage of SOX2+ progenitors (RG) that incorporated BrdU over two days in slice culture (Extended Data Fig. 9). For replication we focused on CP673451, which exhibits the greatest selectivity for PDGFRβ over other receptors[22] and caused the greatest reduction in SOX2+BrdU+ cells among tested inhibitors (Extended Data Fig. 9). PDGFRß inhibition by CP673451 in GW17.5 human neocortical slice cultures reduced the number of RG and intermediate progenitors (IP) that incorporated BrdU by >50%, affecting progenitors in the

Author Manuscript Author Manuscript Author Manuscript Author Manuscript

VZ and SVZ (Fig. 4a-b). The percentage of progenitor cells co-staining with cleaved caspase-3, an apoptosis marker, was slightly elevated by CP673451, but sufficiently low to attribute reduced BrdU incorporation to cell cycle dysregulation rather than cell death (Fig. 4b). Furthermore, CP673451 treatment of E13.5 mouse cortical slice cultures did not decrease BrdU incorporation or the cycling proportion (Ki67+) of RG or IP populations over multiple time points (Fig. 4b, Extended Data Fig. 9). These results indicate that PDGFRß signaling is required for hRG but not mRG to progress through the cell cycle and expand at a normal rate.

We next investigated whether introducing PDGFD into embryonic mouse cortex, where it is normally absent, could promote mRG proliferation. We injected recombinant-PDGF-DD protein into the lateral ventricles of E13.5 mouse embryos, bypassing the need for PDGFD to be generated and dimerized *in vivo*, and analyzed the number and spatial distribution of SOX2+ progenitors at E15.5 in lateral cortex. Relative to vehicle, PDGF-DD increased the proportion of RG (SOX2+/DAPI+) in lateral cortex by ∼10% (Fig. 4c-d). Furthermore, PDGF-DD induced a modest subventricular shift in the distribution of mRG in the developing cortical wall (Fig. 4d). These effects were not observed in dorsomedial cortex, where PDGFRβ was not detected in RG (Fig. 4c-d, Extended Data Fig. 8).

To test if mRG can respond to PDGFRβ activation, we ectopically expressed two forms of constitutively active PDGFRβ (PDGFRβ:D850V [homologous to human D849V[23]] or the TEL-PDGFRβ[24] fusion protein) in mRG by *in utero* electroporation at E13.5. By E15.5, expression of PDGFRβ:D850V approximately doubled the proportion of SOX2+ or Ki67+ progenitors among electroporated (GFP+) cells and dramatically dispersed SOX2+ progenitors in the basal direction (Fig 4e-f; Extended Data Fig. 9). Similar but less dramatic effects were observed following TEL-PDGFRβ electroporation (Extended Data Fig. 9). These results indicate that PDGFRβ signaling in mRG functions analogously to its known role as an oncogenic pathway that promotes proliferation and epithelial-mesenchymal transition[20]. We therefore propose that physiological levels of PDGFD/PDGFRβ signaling in hRG may contribute to the proliferation and subventricular dispersion of neural progenitors that characterizes OSVZ formation[4, 5].

Mouse studies have demonstrated that the size and shape of cerebral cortex depend on precise regulation of molecular pathways controlling RG proliferation and differentiation[1, 2]. While many of these pathways are likely to be conserved in humans, mouse studies alone cannot reveal uniquely human aspects of cortical development[25-30]. By analyzing human tissue as a starting point, we found that PDGFD/PDGFRß signaling is required for normal RG proliferation in developing human but not mouse neocortex, and is sufficient to promote some “humanizing” characteristics in mouse. Our analysis has also identified other genes that likely contribute to differences between human and mouse cortical development. *BMP7*, another secreted growth factor, was predicted and validated to be expressed by hRG but not mRG (Fig. 2d, Extended Data Fig. 6), raising the intriguing possibility that local production of growth factors by hRG may be necessary to support the expanded germinal region and progenitor heterogeneity of developing human neocortex. We anticipate that the analytical and experimental strategies described here will help determine the extent to which these and

Author Manuscript Author Manuscript Author Manuscript Author Manuscript

other pathways are shared among primates or uniquely required for human cortical development.

Methods

Detailed descriptions of all experimental and bioinformatic procedures are provided in Supplementary Information.

Extended Data

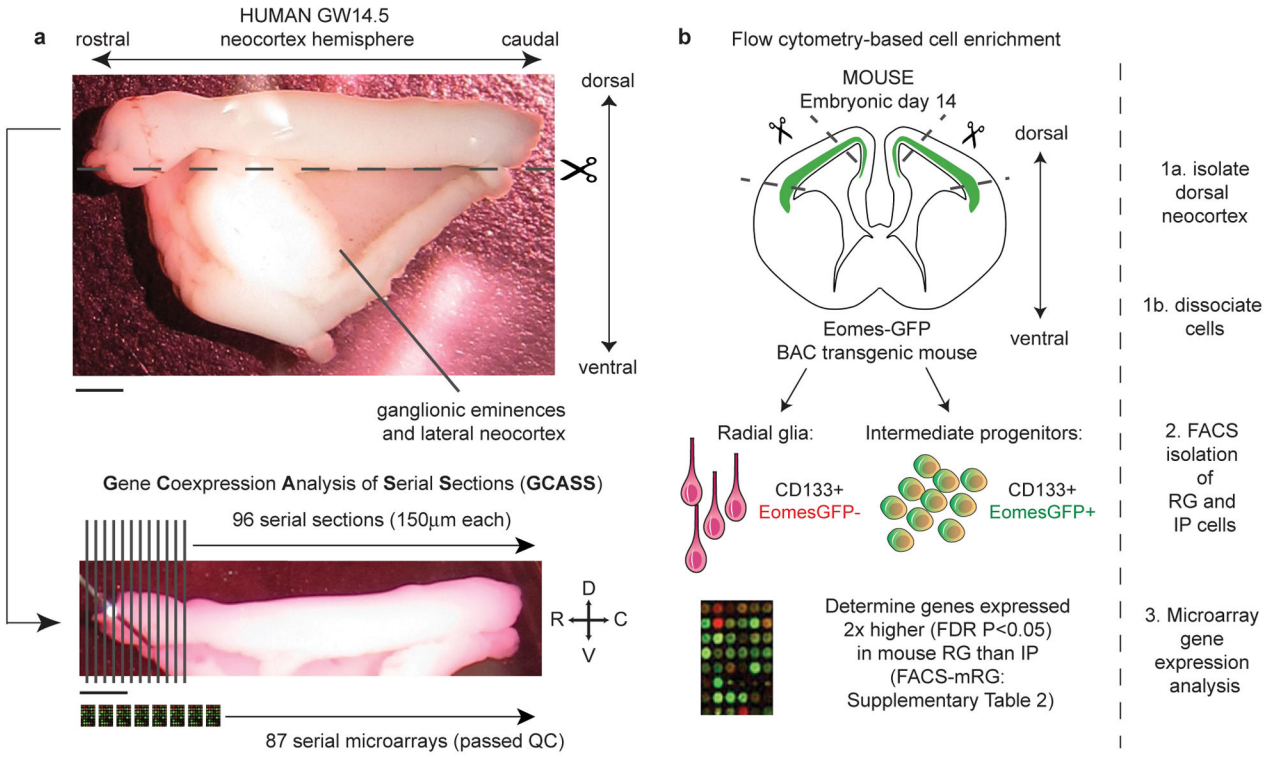

Extended Data Figure 1. Human brain dissection for GCASS and schematic for generation of FACS-mRG dataset

a, Top: To generate the GCASS dataset, an almost-intact prenatal human telencephalic hemisphere (GW14.5) was microdissected to separate the dorsal telencephalon from the ventral telencephalon (including medial and lateral ganglionic eminences). Bottom: The dorsal fragment was flash-frozen and serially sectioned (150 μm) for transcriptional profiling with Illumina HT-12 v4 Beadchip microarrays (scale bars 2.5 mm). **b,** To generate the FACS-mRG dataset, dorsal neocortices of Eomes:GFP mouse embryos were microdissected, pooled (n = 3 litters, 5-8 pooled embryos per litter), dissociated, and FACS-sorted according to the gating scheme depicted to isolate RG and IP cells. Transcriptional profiling of the resultant populations was performed using Illumina mouseRef-8 v1.0 Beadchip microarrays.

Author Manuscript Author Manuscript Author Manuscript Author Manuscript

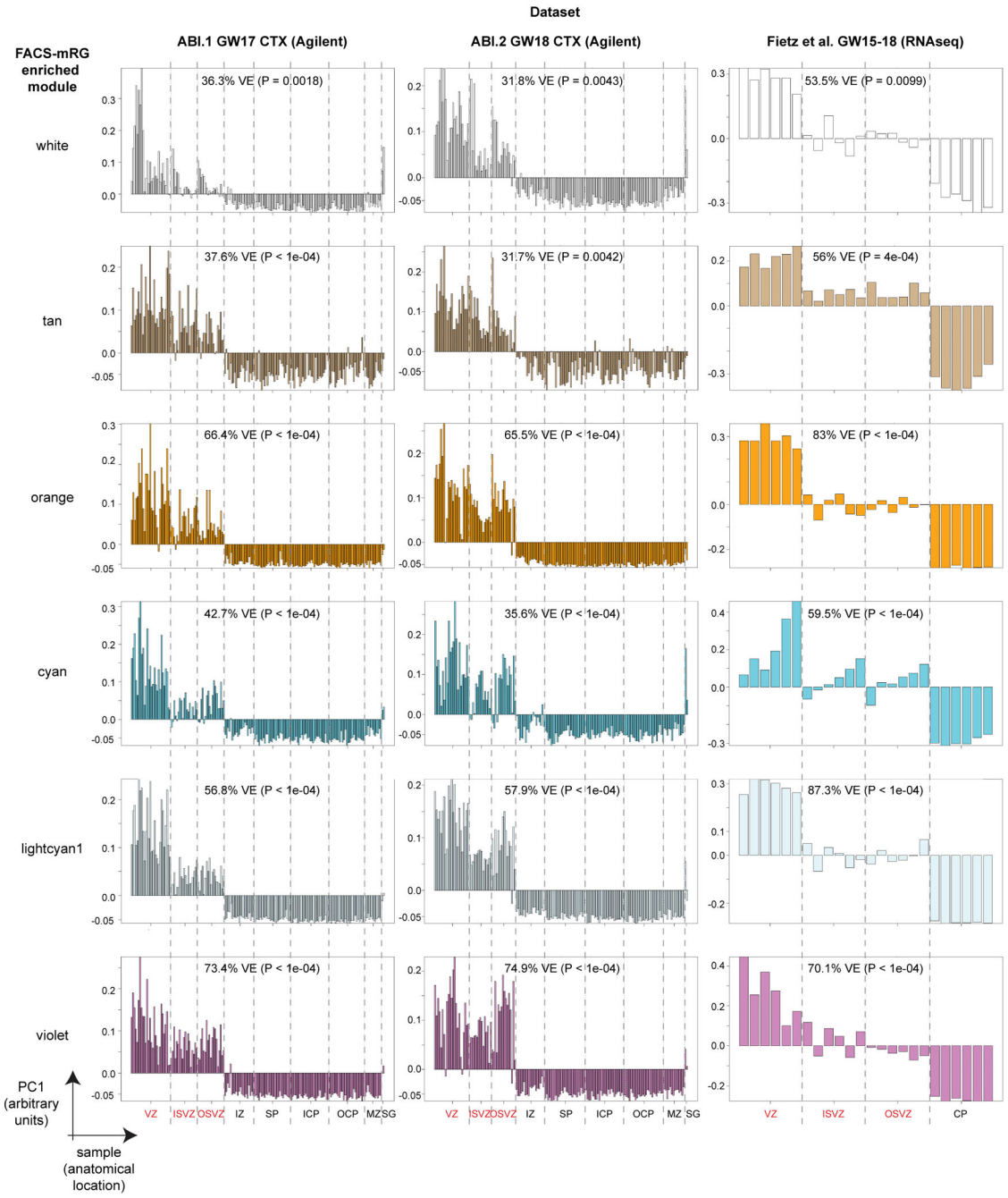

Extended Data Figure 2. Genes comprising the six RG coexpression modules identified by GCASS are expressed in a manner consistent with the known distribution of RG in developing human neocortex

Six candidate hRG gene coexpression modules (Fig. 1d) were superimposed on three independent gene expression datasets generated from laser-microdissected samples from prenatal human cortex: ABI.1[13] (GW17), ABI.2[13] (GW18), and Fietz et al.[12] (GW15-18) (as listed in Extended Data Table 1). The characteristic expression patterns of the superimposed modules were summarized by singular value decomposition; the first principal component (PC1) for each module in each dataset is shown. In all cases, PC1 revealed substantially

Author Manuscript Author Manuscript Author Manuscript Author Manuscript

higher expression levels for these genes in germinal zones (VZ, ISVZ, and OSVZ, highlighted in red) vs. non-germinal zones (IZ, SP, ICP, OCP, CP, MZ, SG). Permutation analysis indicated that the percent variance explained (VE) by PC1 of each superimposed module was significantly greater than expected by chance (n = 10,000 permutations). VZ: ventricular zone, ISVZ: inner subventricular zone, OSVZ: outer subventricular zone, IZ: intermediate zone, SP: subplate, ICP: inner cortical plate, OCP: outer cortical plate, CP: cortical plate, MZ: marginal zone, SG: subpial granular layer, GW: gestational week, CTX: cortex.

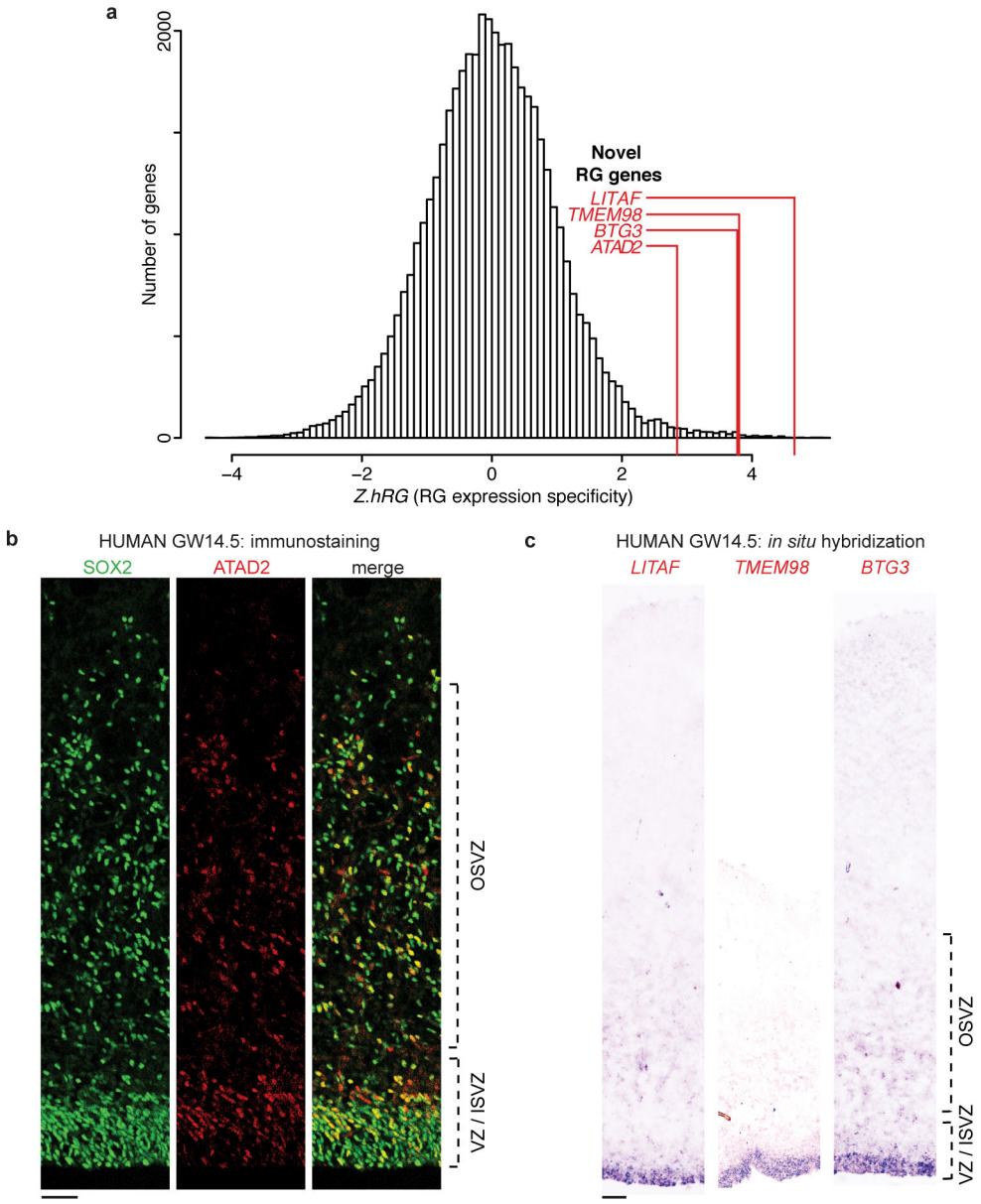

Extended Data Figure 3. GCASS successfully predicts novel markers of neocortical hRG

Author Manuscript Author Manuscript Author Manuscript Author Manuscript

a, Genome-wide distribution of predicted GW14.5 neocortical hRG expression specificity (*Z.hRG*). Red lines: predicted RG genes (validated in **b-c**). **b-c,** Immunostaining and *in situ* hybridization in GW14.5 human neocortex confirms RG expression specificity for novel candidate markers predicted in (**a**) (**b,** scale bar 50 μm; **c,** scale bar 100 μm). Analyzed tissue sections were independent from the sample used for microarray analysis (Fig. 1a). VZ: ventricular zone, (I/O)SVZ: (inner/outer) subventricular zone.

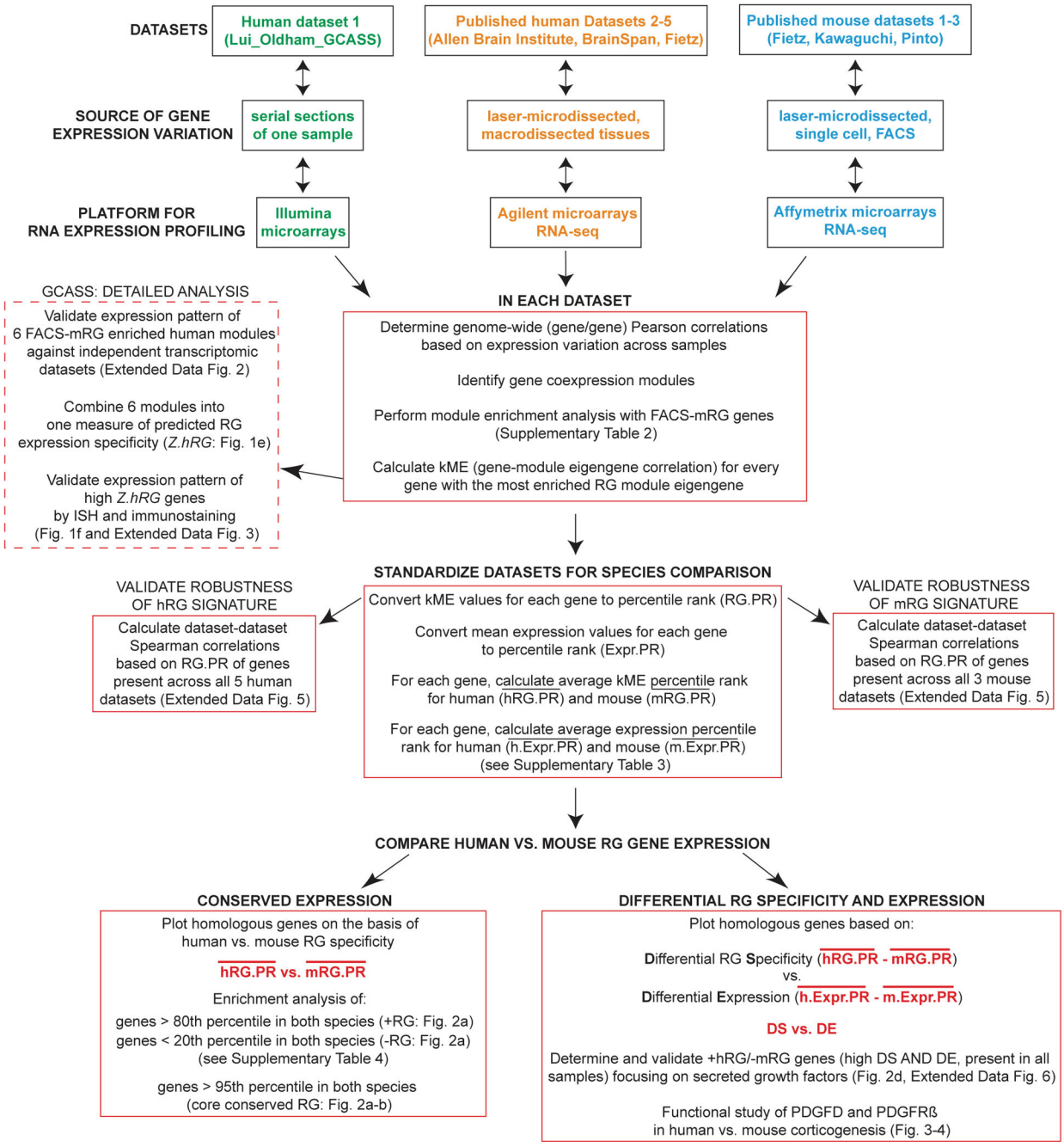

Extended Data Figure 4. Workflow of bioinformatic procedures and experimental rationale for the entire study

Author Manuscript Author Manuscript Author Manuscript Author Manuscript

The bioinformatic component of this study sought to identify a homologous gene coexpression signature for human and mouse RG cells that is robust across multiple sampling strategies/technology platforms and can be normalized to facilitate comparisons within and between species. This pipeline illustrates the steps that were taken to identify, integrate, and compare RG gene coexpression signatures in eight transcriptomic datasets generated from prenatal human and mouse neocortex.

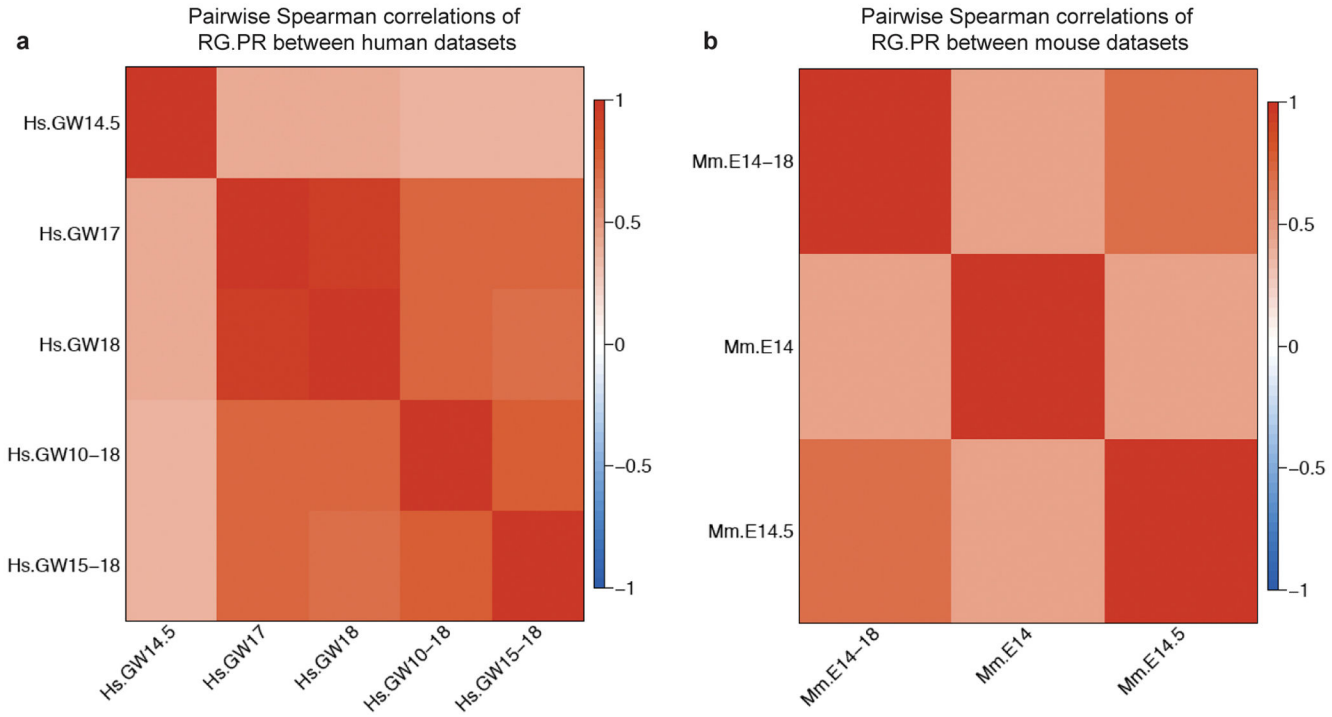

Extended Data Figure 5. Genome-wide predictions of expression specificity for hRG and mRG are robust across independent datasets

a-b, Heat maps of Spearman correlation coefficients for predicted RG expression specificity (RG.PR) over 10,929 genes present in all five human datasets (**a**) and 10,649 genes present in all three mouse datasets (**b**) (as indicated in columns BE and BI in Supplementary Table 3). Datasets are denoted by the sample ages listed in Extended Data Table 1, though factors besides age also contribute to the observed correlations (e.g. choice of technology platform, sample preparation strategy, etc.). E: embryonic, GW: gestational week.

Author Manuscript Author Manuscript Author Manuscript Author Manuscript

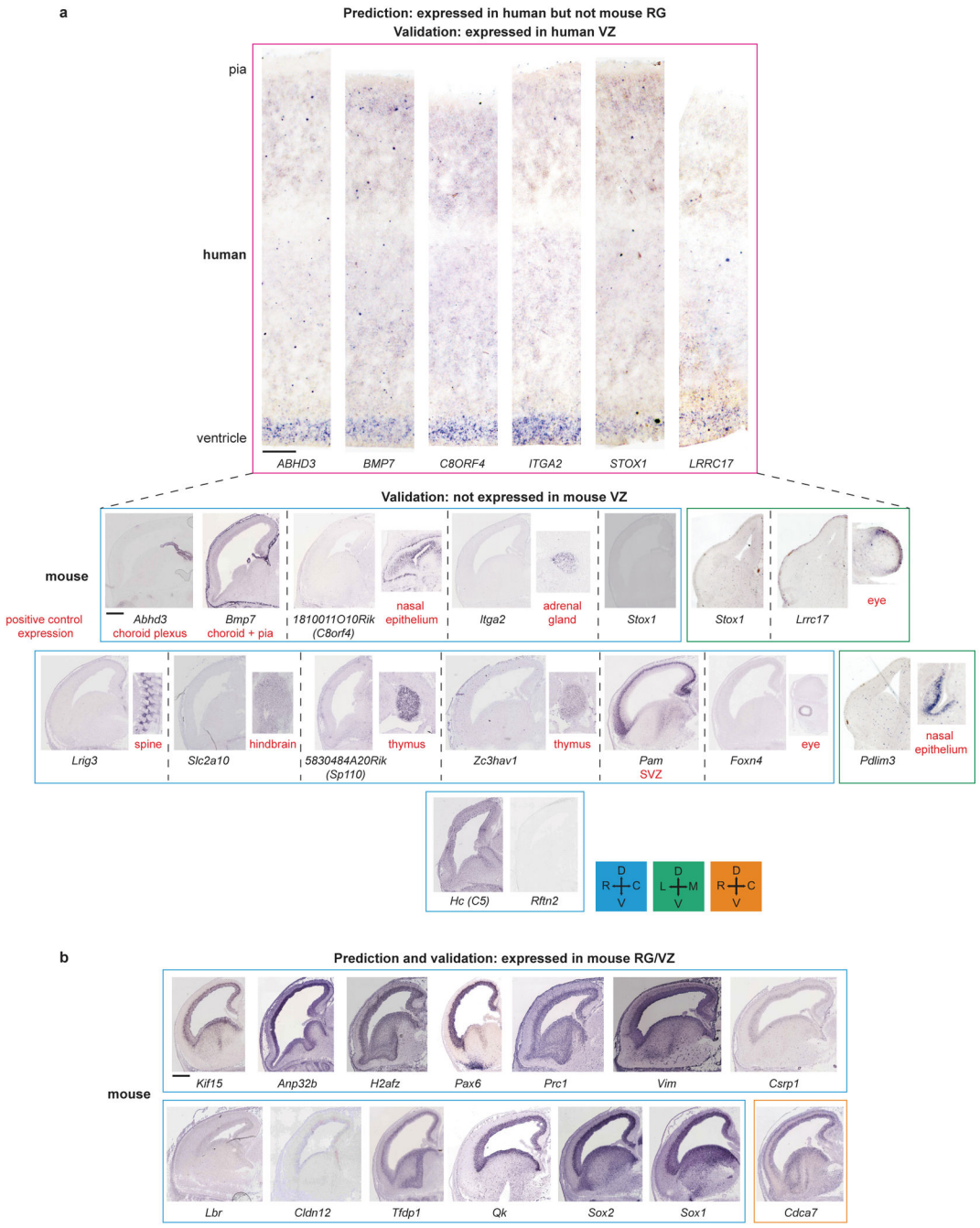

Extended Data Figure 6. *In situ* hybridization (ISH) validates predicted presence or absence of gene expression in hRG and mRG

a, Pink: human *in situ* probes for 6 genes predicted to be expressed by hRG but not mRG were generated and hybridized in GW15 human neocortical tissue to validate predicted hRG expression (human scale bar 200 μm). Blue (Eurexpress[21]: http://www.eurexpress.org/ee/): *in situ* hybridizations for 13 genes predicted to be expressed by hRG but not mRG reveal no expression by mRG in E14.5 mouse cortex. Green: mouse *in situ* probes for 3 genes predicted to be expressed by hRG but not mRG were generated and revealed no expression

Author Manuscript Author Manuscript Author Manuscript Author Manuscript

by mRG (E13.5). Positive control expression in cells other than RG are labeled in red. **b,** Expression patterns of genes predicted to be expressed by mRG (i.e. those with the highest $\overline{\text{mRG.PR}}$ values in Supplementary Table 3) are shown as further validation (Blue [E14.5, Eurexpress[21]: http://www.eurexpress.org/ee/]; Orange [E14.5, GenePaint[31]: http://www.genepaint.org]; mouse scale bars ~500 μm). One other gene in the top 15, *Cks2*, is not shown, but was validated by Ajioka et al., 2006[32].

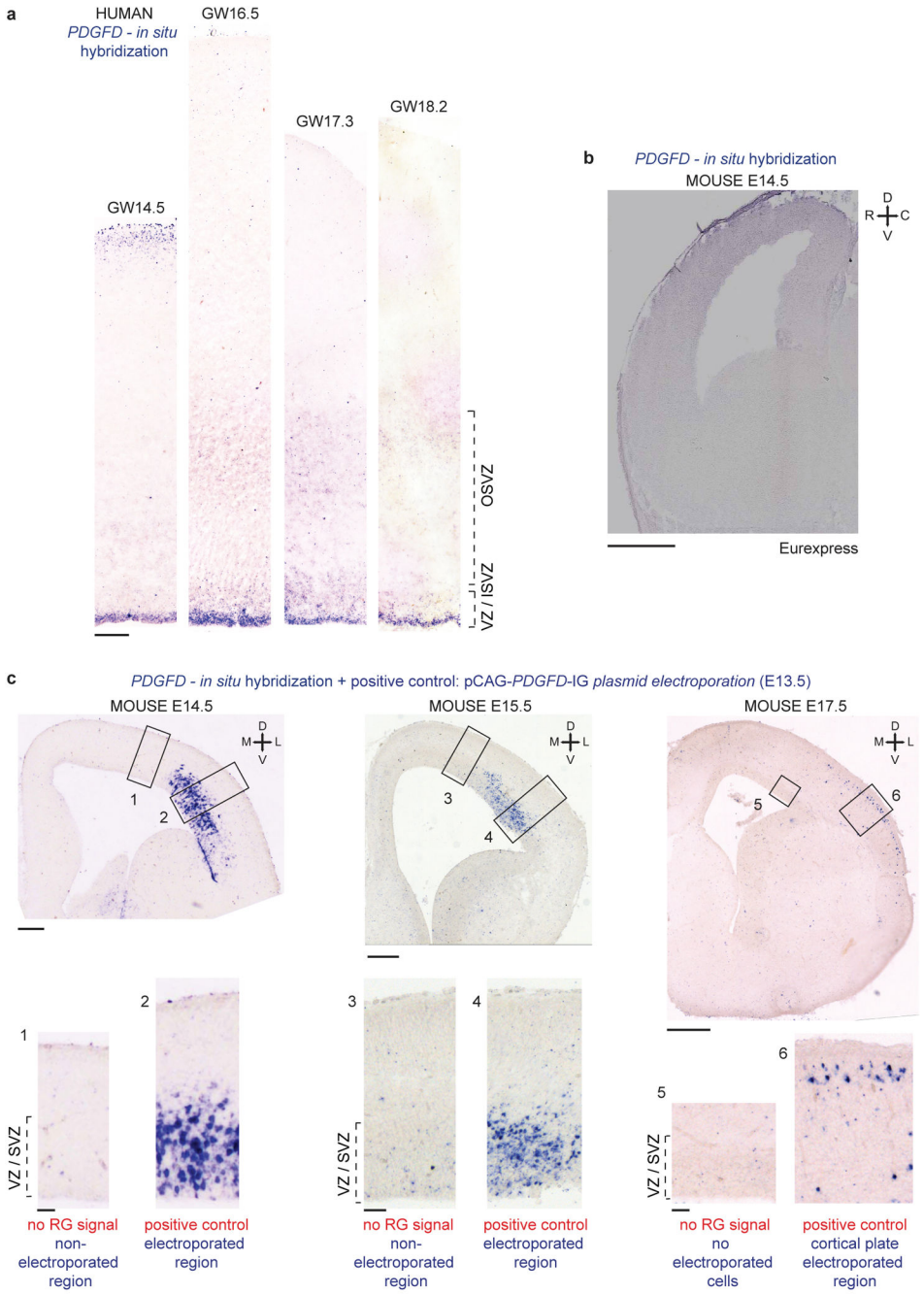

Extended Data Figure 7. *PDGFD* is expressed by neocortical RG during neurogenesis in humans, but not mice

Author Manuscript Author Manuscript Author Manuscript Author Manuscript

a, *In situ* hybridization of *PDGFD* in GW14.5, 16.5, 17.3, and 18.2 human neocortex demonstrates consistent expression in RG across multiple ages (scale bar 200 μm). **b,** *In situ* hybridization of *Pdgfd* in E14.5 mouse (Eurexpress[21]: http://www.eurexpress.org/ee/) demonstrates lack of expression (scale bar ~500 μm). **c,** To demonstrate the lack of *Pdgfd* expression in mouse neocortex across multiple ages, a pCAG-*PDGFD*-IG expression plasmid was electroporated into the mouse VZ at E13.5 as an internal positive control and harvested at E14.5, E15.5, or E17.5. At E14.5 and E15.5, *Pdgfd* (blue signal) is seen only in the electroporated region in the ventricular zone (scale bar 200 μm, inset scale bar 50 μm). At E17.5, *Pdgfd* is in the cortical plate, and not in the ventricular zone or anywhere else (scale bar 500 μm, inset scale bar 50 μm). VZ: ventricular zone, (I/O)SVZ: (inner/outer) subventricular zone.

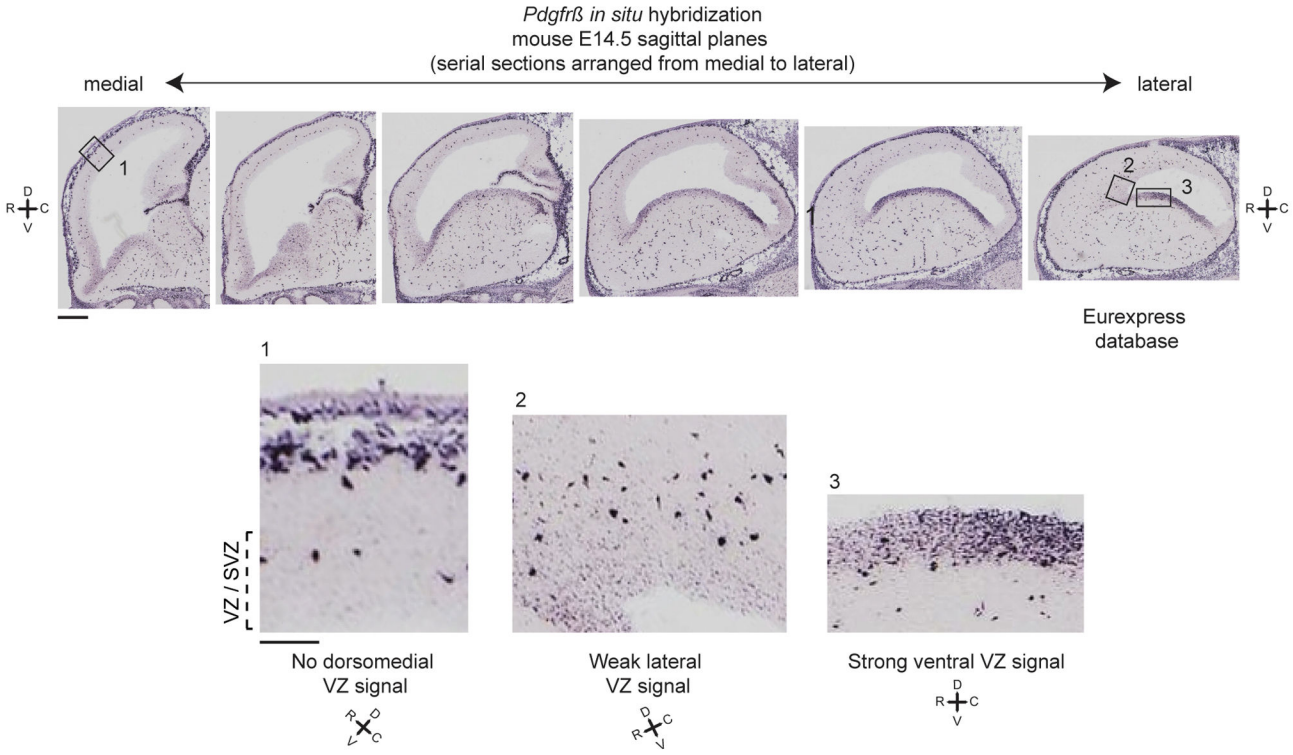

Extended Data Figure 8. *Pdgfrβ* is strongly expressed by ventral RG and weakly expressed by lateral RG in mice

In situ hybridization of *Pdgfrβ* in sagittal sections through the mouse forebrain (E14.5) across a medial-lateral axis (Eurexpress[21]: http://www.eurexpress.org/ee/) demonstrates progenitor expression in the ventral germinal regions. This expression extends into the dorsal cortex in the lateral aspect of the brain, but is not widespread. In contrast, no progenitor expression is detected in dorsomedial cortex (scale bar 500 μm, inset scale bar 100 μm). Expression is also detected in the pia and vascular pericytes. VZ: ventricular zone, SVZ: subventricular zone.

Author Manuscript Author Manuscript Author Manuscript Author Manuscript

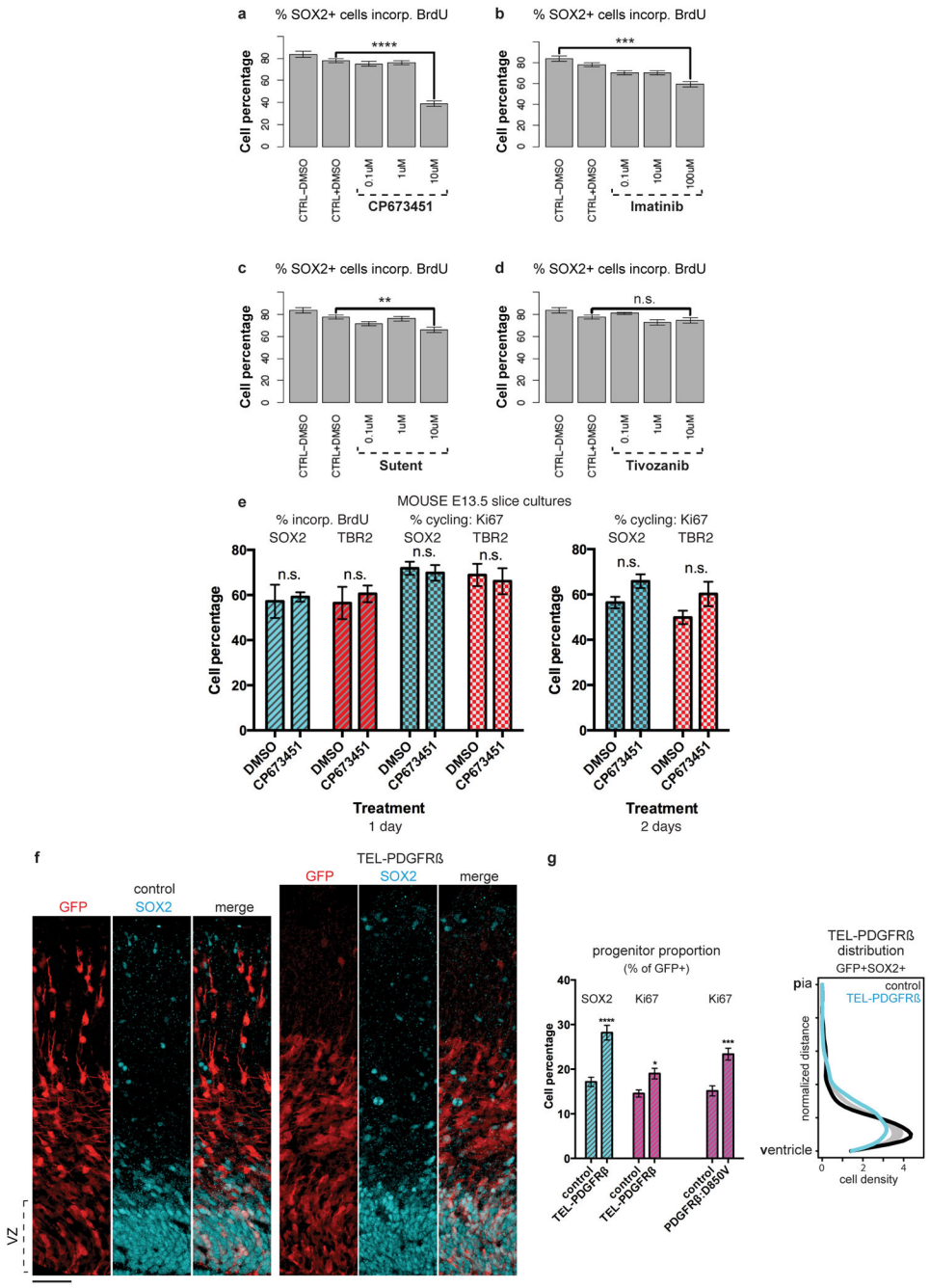

Extended Data Figure 9. Manipulation of PDGFRß signaling in human and mouse neocortex

a-d, Chemical blockade of PDGFRß signaling in cultured slices of GW14.5 human neocortex impairs RG cell cycle progression. Four pharmacological inhibitors of PDGFRß signaling were screened at different concentrations to determine their effects on RG proliferation in cultured slices of GW17.5 human neocortex (2 days). Slices were treated with BrdU for the duration of the experiment and RG proliferation was quantified as the fraction of SOX2+ cells that incorporated BrdU following treatment with inhibitor or vehicle. Statistical significance was assessed with the Wilcoxon rank sum test using the

Author Manuscript Author Manuscript Author Manuscript Author Manuscript

`wilcox.test`

R function with default settings. Images derived from ≥3 slices in each condition. Control + DMSO n = 18; control no DMSO n = 9; CP673451 all conc. n = 9; Sutent all conc. n = 6; Imatinib [0.1μM, 10μM] n = 9, [100μM] n = 6; Tivozanib [1μM, 10μM] n = 9, [0.1μM] n = 6. Significance indicated by: n.s. P > 0.05, **P ≤ 0.01, ***P ≤ 0.001, ****P ≤ 0.0001. **e,** Slice cultures of E13.5 mouse neocortex were treated with BrdU and DMSO (control) or a pharmacological inhibitor of PDGFRß signaling (CP673451) for 1 or 2 d (slices from at least 3 independent litters). RG (SOX2+) or IP (TBR2+) cell proliferation was assessed as the fraction each population that incorporated BrdU or was Ki67+ (1d: n = 10 [DMSO] vs. n = 9 [CP673451]; 2d: n = 11 [DMSO] vs. n = 9 [CP673451]). This experiment serves as a negative control to compare with the human. **f,** Ectopic PDGFRß signaling promotes RG identity in E13.5 mouse neocortex. *In utero* electroporation of constitutively active TEL-PDGFRβ[24] was compared with control (mouse E13.5-E15.5) and assessed for the proportion and distribution of SOX2+ RG cells or Ki67+ progenitors (out of GFP+) in the cortical wall (quantified in **g**: at least n = 3 slices per embryo from 2 independent litters, n = 15 [control]; n = 18 [TEL-PDGFRβ] or [PDGFRβ:D850V]; scale bar 50 μm). Ki67+GFP+ cell quantification following PDGFRβ:D850V[23] electroporation was performed in a similar fashion and is also shown. The spatial distributions of RG (GFP+SOX2+) in the cortical wall were assessed by quantitative image analysis (spanning ventricle to pia). The grey band delineates a 95% confidence interval for a test of equal univariate densities based on 10,000 permutations. All error bars represent mean +/- s.e.m. Statistical significance for the effects of treatment was calculated by ANOVA of multiple linear regression while controlling for individual (**e**) and litter (**f**) variability (significance indicated by: n.s. P > 0.05, *P ≤ 0.05, **P ≤ 0.01, ***P ≤ 0.001, ****P ≤ 0.0001). VZ: ventricular zone.

Extended Data Table 1
Characteristics of additional gene expression datasets analyzed in the present study

Unsupervised gene coexpression analysis was performed for each dataset using the same parameters, followed by unbiased enrichment analysis with the FACS-mRG gene set (Supplementary Table 2; Extended Data Fig. 1). “mRG enrichment P-value” denotes the P-value (Fisher's exact test) for the module with the most significant enrichment in each dataset. ABI: Allen Institute for Brain Science, CTX: cortex, E: embryonic, FACS: fluorescence-activated cell sorting, GW: gestational week, LMD: laser-microdissection, Macro: macrodissection, OR: odds ratio [95% confidence interval].

Dataset	Platform	Species	CTX prep	Age	Samples	mRG inrichment P-value	OR
ABI.1[13]	Agilent	Human	LMD	GW17	179	2.6e-39	7.2 [5.5-9.5]
ABI.2[13]	Agilent	Human	LMD	GW18	168	9.7e-35	7.5 [5.6-10.0]
BrainSpan[17]	RNAseq	Human	Macro	GW10-18	107	2.0e-47	9.2 [6.9-12.1]
Fietz et al.[12]	RNAseq	Human	LMD	GW15-18	24	1.3e-39	8.4 [6.3-11.1]
Fietz et al.[12]	RNAseq	Mouse	LMD	E14.5	15	1.3e-73	12.5 [9.6-16.4]
Kawaguchi et al.[18]	Affymetrix	Mouse	Single Cell	E14	70	3.1e-34	59.0 [34.2-100.6]

Author Manuscript Author Manuscript Author Manuscript Author Manuscript

Dataset	Platform	Species	CTX prep	Age	Samples	mRG inrichment P-value	OR
Pinto et al.[19]	Affymetrix	Mouse	FACS	E14-18	17	7.8e-46	20.7 [14.7-29.0]

Supplementary Material

Refer to Web version on PubMed Central for supplementary material.

Acknowledgments

We thank the staff at San Francisco General Hospital Women's Options Center for their consideration in allowing access to donated human prenatal tissue. We thank Joe DeYoung and the staff at the Southern California Genotyping Consortium at the University of California Los Angeles for microarray data generation. We are grateful to Alisha Holloway for her critical reading of the manuscript, and also thank W. Walantus, S. Wang, Y. Wang and other University of California San Francisco personnel for technical and administrative support. We thank C. Stiles and D. Rowitch for the TEL-PDGFRβ construct. Due to space limitations, we apologize that many primary and historical publications have not been cited. This work was supported by grants from the N.I.H., the Bernard Osher Foundation, a California Institute for Regenerative Medicine Predoctoral Fellowship for J.H.L. (TG2-01153), a Damon Runyon Foundation Postdoctoral Fellowship for A.A.P. (DRG-2013), and the University of California San Francisco Program for Breakthrough Biomedical Research, which is funded in part by the Sandler Foundation (M.C.O). The contents of this publication are solely the responsibility of the authors and do not necessarily represent the official views of the California Institute for Regenerative Medicine or any other agency of the State of California.

References

1. Rakic P. Evolution of the neocortex: a perspective from developmental biology. Nat Rev Neurosci. 2009; 10(10):724. [PubMed: 19763105]
2. Lui JH, Hansen DV, Kriegstein AR. Development and evolution of the human neocortex. Cell. 2011; 146(1):18. [PubMed: 21729779]
3. Smart IH, et al. Unique morphological features of the proliferative zones and postmitotic compartments of the neural epithelium giving rise to striate and extrastriate cortex in the monkey. Cereb Cortex. 2002; 12(1):37. [PubMed: 11734531]
4. Hansen DV, Lui JH, Parker PR, Kriegstein AR. Neurogenic radial glia in the outer subventricular zone of human neocortex. Nature. 2010; 464(7288):554. [PubMed: 20154730]
5. Fietz SA, et al. OSVZ progenitors of human and ferret neocortex are epithelial-like and expand by integrin signaling. Nat Neurosci. 2010
6. Bergsten E, et al. PDGF-D is a specific, protease-activated ligand for the PDGF beta-receptor. Nat Cell Biol. 2001; 3(5):512. [PubMed: 11331881]
7. LaRochelle WJ, et al. PDGF-D, a new protease-activated growth factor. Nat Cell Biol. 2001; 3(5): 517. [PubMed: 11331882]
8. Rakic P. Specification of cerebral cortical areas. Science. 1988; 241(4862):170. [PubMed: 3291116]
9. Oldham, MC. Transcriptomics: from differential expression to coexpression. In: Coppola, G., editor. The OMICs: Applications in Neuroscienc. Vol. 1. Oxford University Press; Oxford: 2014. p. 85
10. Oldham MC. Functional organization of the transcriptome in human brain. Nat Neurosci. 2008; 11(11):1271. [PubMed: 18849986]
11. Workman AD, et al. Modeling transformations of neurodevelopmental sequences across mammalian species. J Neurosci. 2013; 33:7368. [PubMed: 23616543]
12. Fietz SA, et al. Transcriptomes of germinal zones of human and mouse fetal neocortex suggest a role of extracellular matrix in progenitor self-renewal. Proc Natl Acad Sci U S A. 2012; 109(29): 11836. [PubMed: 22753484]
13. Miller JA, et al. Transcriptional landscape of the prenatal human brain. Nature. 2014
14. Horvath S, Dong J. Geometric interpretation of gene coexpression network analysis. PLoS Comput Biol. 2008; 4(8):e1000117. [PubMed: 18704157]

Author Manuscript Author Manuscript Author Manuscript Author Manuscript

15. Oldham MC, Horvath S, Geschwind DH. Conservation and evolution of gene coexpression networks in human and chimpanzee brains. Proc Natl Acad Sci U S A. 2006; 103(47):17973. [PubMed: 17101986]
16. Zhang B, Horvath S. A general framework for weighted gene co-expression network analysis. Stat Appl Genet Mol Biol. 2005; 4 Article17.
17. BrainSpan. http://www.brainspan.org/rnaseq/search/index.html
18. Kawaguchi A, et al. Single-cell gene profiling defines differential progenitor subclasses in mammalian neurogenesis. Development. 2008; 135(18):3113. [PubMed: 18725516]
19. Pinto L, et al. Prospective isolation of functionally distinct radial glial subtypes--lineage and transcriptome analysis. Mol Cell Neurosci. 2008; 38(1):15. [PubMed: 18372191]
20. Wang Z, et al. Emerging roles of PDGF-D signaling pathway in tumor development and progression. Biochim Biophys Acta. 2010; 1806(1):122. [PubMed: 20434526]
21. Diez-Roux G, et al. A high-resolution anatomical atlas of the transcriptome in the mouse embryo. PLoS Biol. 2011; 9(1):e1000582. [PubMed: 21267068]
22. Roberts WG, et al. Antiangiogenic and antitumor activity of a selective PDGFR tyrosine kinase inhibitor, CP-673,451. Cancer Res. 2005; 65(3):957. [PubMed: 15705896]
23. Magnusson PU, et al. Platelet-derived growth factor receptor-beta constitutive activity promotes angiogenesis in vivo and in vitro. Arterioscler Thromb Vasc Biol. 2007; 27(10):2142. [PubMed: 17656670]
24. Golub TR, Barker GF, Lovett M, Gilliland DG. Fusion of PDGF receptor beta to a novel ets-like gene, tel, in chronic myelomonocytic leukemia with t(5;12) chromosomal translocation. Cell. 1994; 77(2):307. [PubMed: 8168137]
25. McLean CY, et al. Human-specific loss of regulatory DNA and the evolution of human-specific traits. Nature. 2011; 471(7337):216. [PubMed: 21390129]
26. Bae BI, et al. Evolutionarily dynamic alternative splicing of GPR56 regulates regional cerebral cortical patterning. Science. 2014; 343(6172):764. [PubMed: 24531968]
27. Geschwind DH, Rakic P. Cortical evolution: judge the brain by its cover. Neuron. 2013; 80(3):633. [PubMed: 24183016]
28. Johnson MB, et al. Functional and evolutionary insights into human brain development through global transcriptome analysis. Neuron. 2009; 62(4):494. [PubMed: 19477152]
29. Kang HJ. Spatio-temporal transcriptome of the human brain. Nature. 2011; 478(7370):483. [PubMed: 22031440]
30. Hawrylycz MJ, et al. An anatomically comprehensive atlas of the adult human brain transcriptome. Nature. 2012; 489(7416):391. [PubMed: 22996553]

Author Manuscript Author Manuscript Author Manuscript Author Manuscript

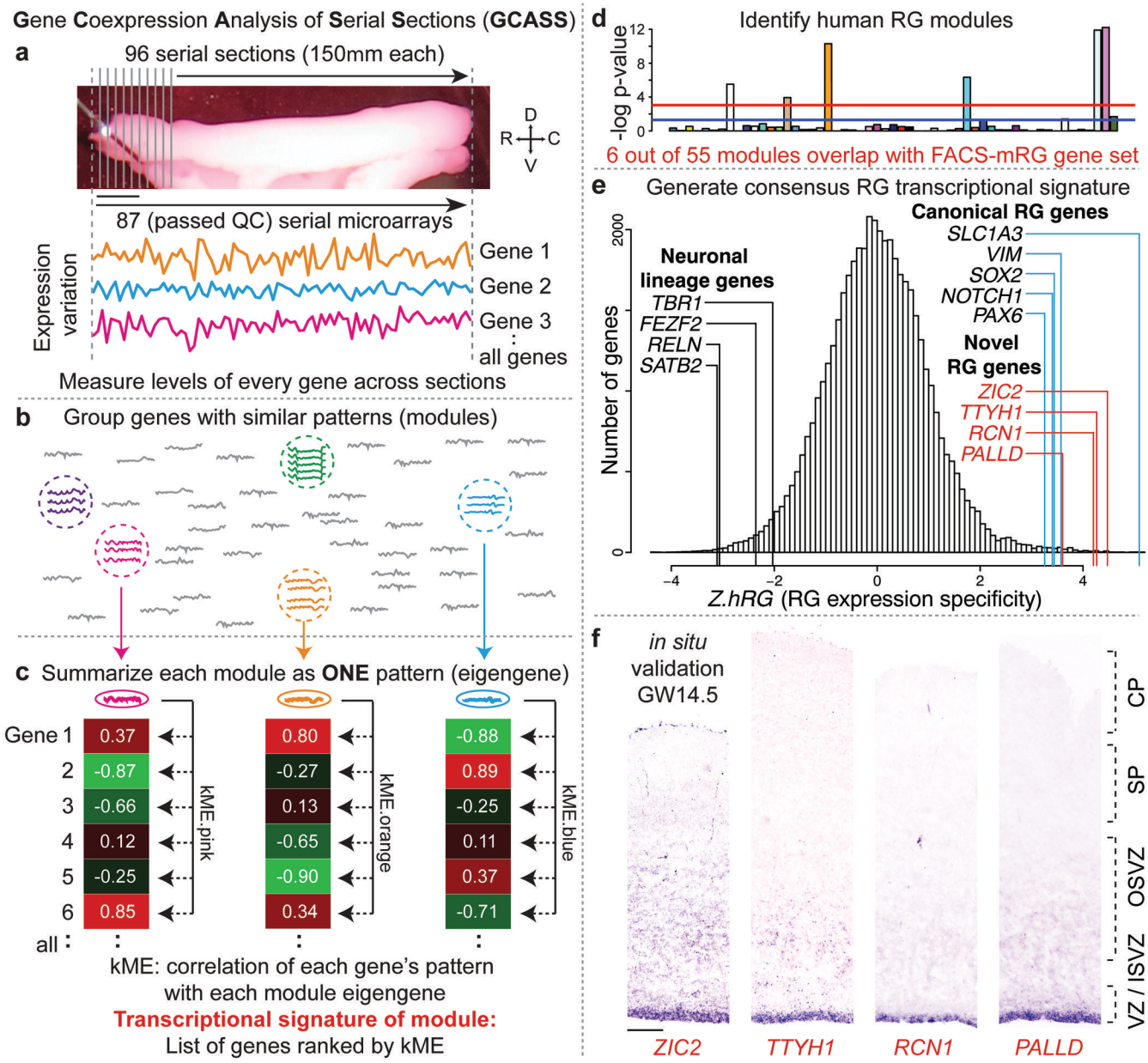

Figure 1. GCASS identifies a transcriptional signature of radial glia (RG) in human neocortex

Left Conceptual framework. **a,** Transcriptional profiling of serial sections (n = 87, Illumina HT12v4 microarrays) from a GW14.5 human neocortical specimen (scale bar 2.5 mm). **b,** Genes with similar expression patterns are grouped into modules, which may reflect cell typespecific gene coexpression[10]. **c,** The transcriptional signature of a module is defined as a list of genes ranked by their correlation to the module eigengene[14]. **Right**: Finding human RG modules. **d,** Six out of 55 modules were significantly enriched (Fisher's exact test) with the FACS-mRG gene set. Blue line: P = .05; red line: P = 9.1e-04 (Bonferroni correction). **e,** Genome-wide distribution of predicted GW14.5 neocortical RG expression specificity (*Z.hRG*) based on enriched modules in **(d). f,** ISH confirms RG expression specificity for

Author Manuscript Author Manuscript Author Manuscript Author Manuscript

novel RG genes from **e** (scale bar 300 μm). (I/O)SVZ: inner/outer subventricular zone, SP: subplate, CP: cortical plate.

Author Manuscript Author Manuscript Author Manuscript Author Manuscript

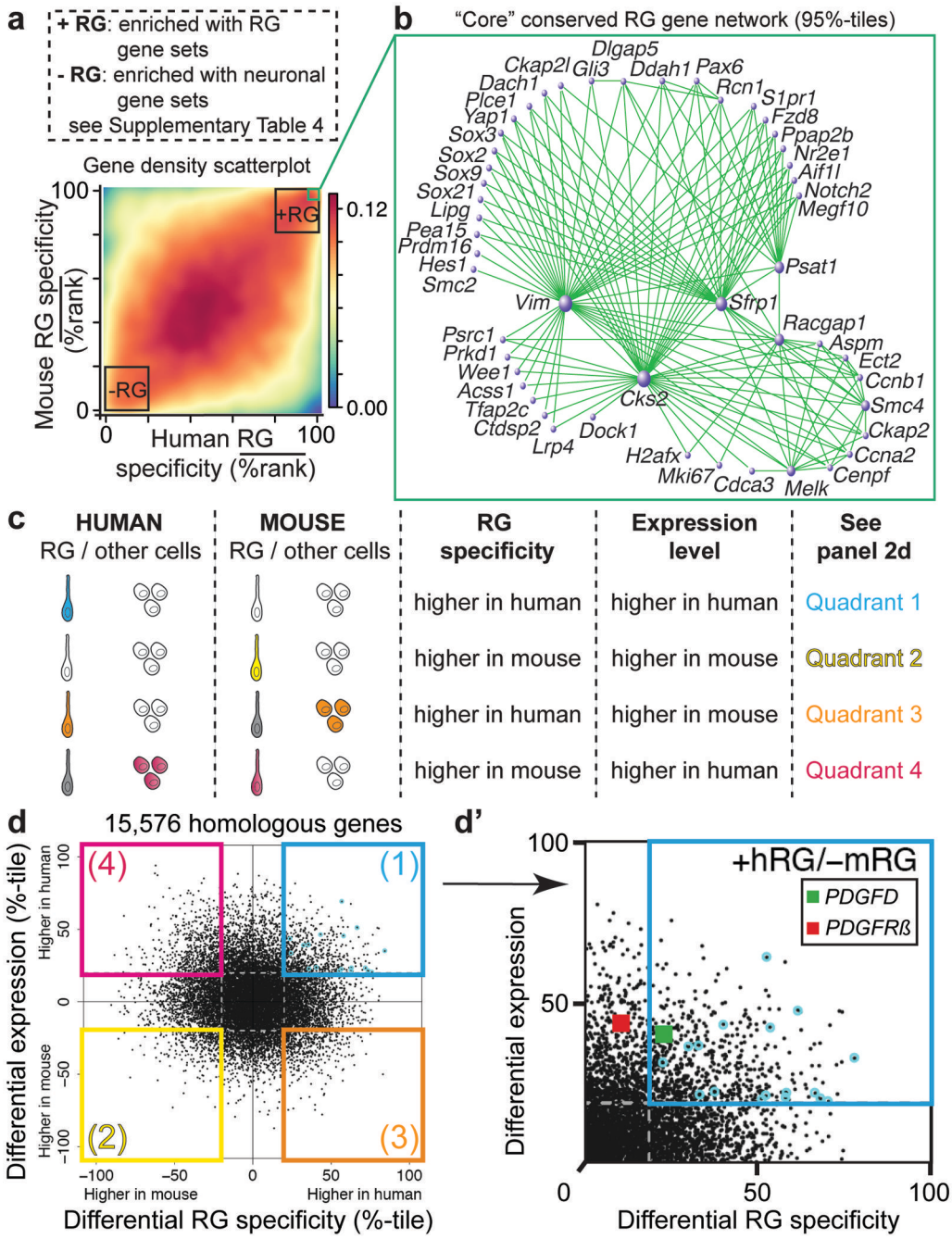

Figure 2. Combined differential RG specificity / differential expression analysis identifies gene expression differences that distinguish neocortical RG between human and mouse

a, Predicted RG expression specificity for 15,576 homologous genes in human and mouse. **b,** The core transcriptional architecture of RG. Node size corresponds to connectivity. **c,** Idealized examples of four types of evolutionary change that could drive differences in predicted hRG and mRG expression specificity. **d,** Comparison of differential RG specificity and differential expression for homologous genes between human and mouse. Dashed grey lines delineate arbitrary thresholds (-20, 20) used to define quadrants (1-4) for enrichment

analyses (Supplementary Table 4). Cyan circles highlight 18 genes predicted to be expressed in hRG but not mRG; one of these encodes the growth factor *PDGFD* (**d',** green square). Its cognate receptor *PDGFRβ* is also highlighted (**d',** red square).

Author Manuscript Author Manuscript Author Manuscript Author Manuscript

Author Manuscript Author Manuscript Author Manuscript Author Manuscript

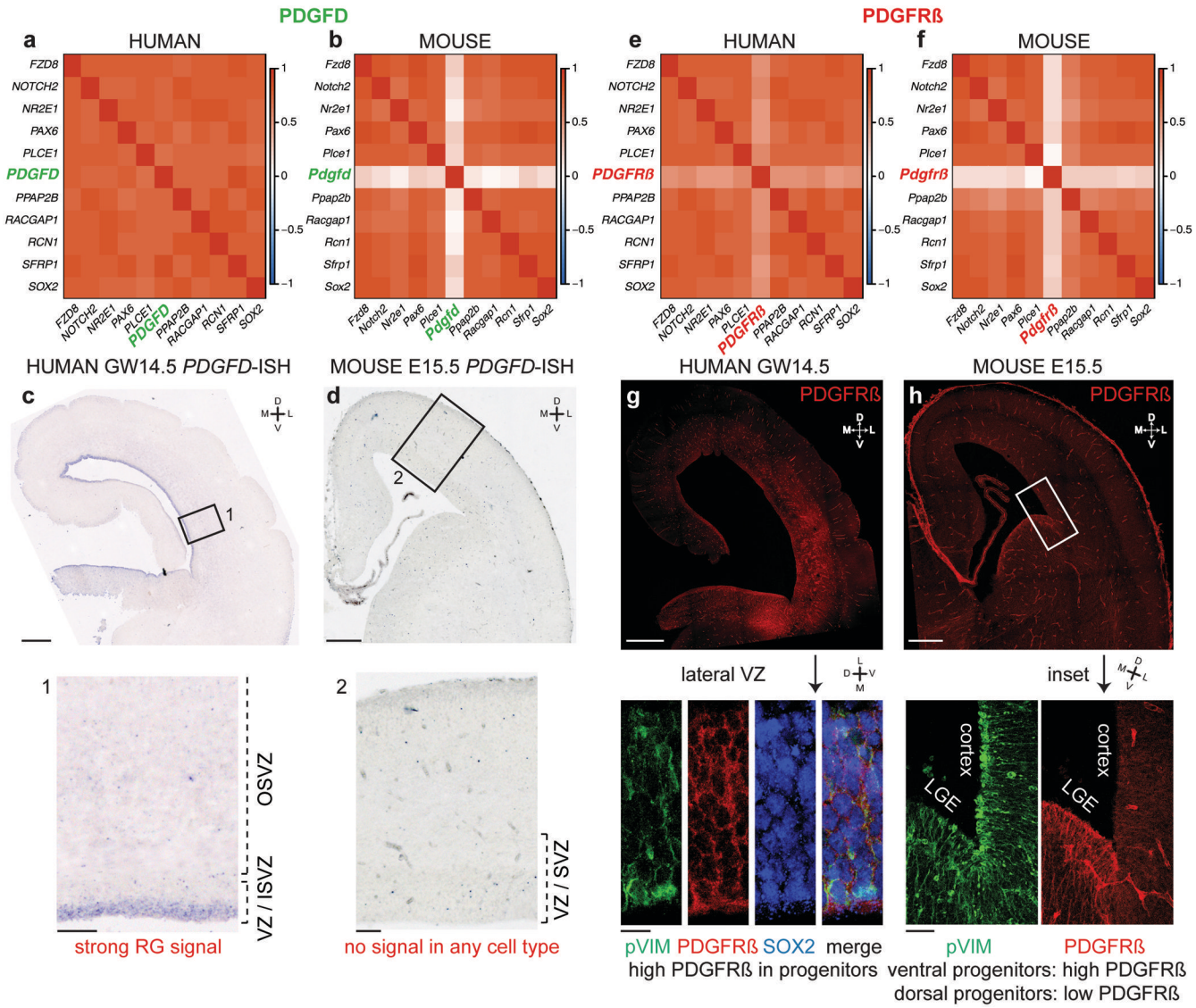

Figure 3. PDGFD and PDGFRß are expressed in human but not mouse dorsal RG

Consensus Pearson correlations among expression levels of *PDGFD* (**a,** human), *Pdgfd* (**b,** mouse), *PDGFRβ* (**e,** human), or *Pdgfrβ* (**f,** mouse) and 10 genes with the highest $\overline{\mathrm{RG.PR}}$ **c-d,** ISH of *PDGFD* in human (**c,** scale bar 1 mm, inset scale bar 200 μm) and mouse neocortex (**d,** scale bar 200 μm, inset scale bar 50 μm). **g,** Immunostaining of PDGFRß in human neocortex (scale bar 1 mm). 63x image of lateral VZ demonstrates co-labeling of PDGFRß with pVIM- and SOX2-expressing RG (scale bar 10 μm). The pia and choroid plexus are absent due to human tissue processing. **h,** Immunostaining of PDGFRß in mouse neocortex (comparison with pVIM in the lateral ganglionic eminence [LGE]; scale bar 250 μm, inset scale bar 50 μm).

Author Manuscript Author Manuscript Author Manuscript Author Manuscript

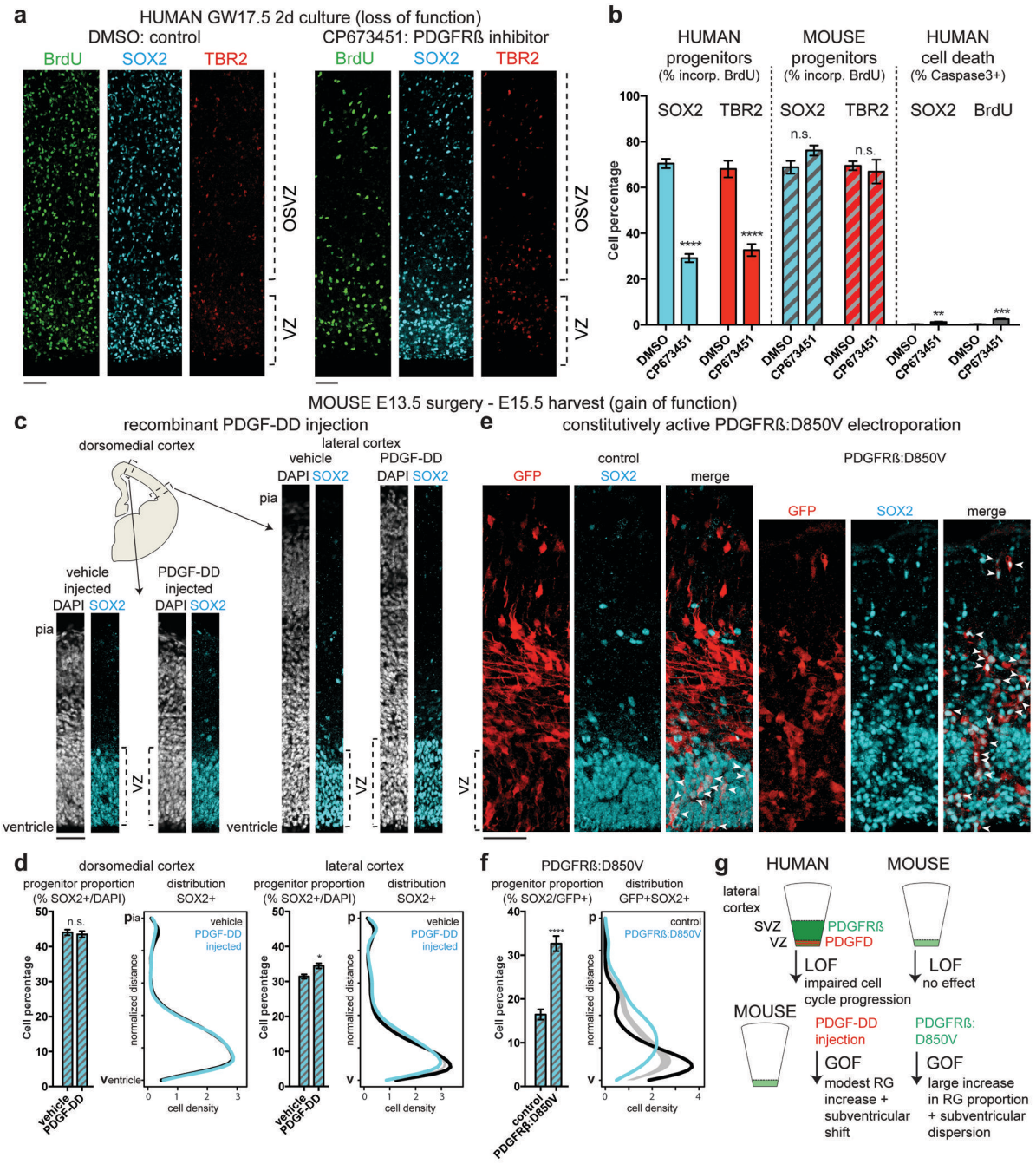

Figure 4. PDGFD/PDGFRß signaling is necessary for normal cell cycle progression of neocortical RG in humans and sufficient to promote RG identity in mice

a, GW17.5 human neocortical slice cultures were treated with BrdU and DMSO (control) or an inhibitor of PDGFRß signaling (CP673451) (scale bar 50 μm). The same experiment was performed in E13.5 mouse neocortical slice cultures (slices from at least 3 individuals/litters per species). **b,** RG (IP) proliferation was quantified as the fraction of SOX2+ (TBR2+) cells that incorporated BrdU after 48 hours. RG slice counts: human (n = 18 [DMSO] vs. n = 17 [CP673451]); mouse (n = 13 [DMSO] vs. n = 11 [CP673451]). IP slice counts: human (n =

Author Manuscript Author Manuscript Author Manuscript Author Manuscript

12 [DMSO] vs. n = 10 [CP673451]); mouse (n = 11 [DMSO] vs. n = 9 [CP673451]). Cell death was quantified in human slices as the fraction of SOX2+ or BrdU+ cells that co-stained for cleaved-caspase 3 (n = 6 [DMSO] vs. n = 7 [CP673451]). **c,** *In utero* intraventricular injection of recombinant human PDGF-DD protein (mouse E13.5-E15.5). Brain tissue was stained for SOX2 and DAPI (scale bar 50 μm). **d,** Quantification of data from **c** in dorsomedial and lateral cortex (at least n = 3 slices per embryo from 5 litters/ experiments [lateral: n = 49 vehicle; n = 47 PDGF-DD; dorsomedial: n = 45 vehicle; n = 39 PDGF-DD]). The distribution of RG in the cortex (from ventricle to pia) was quantified; grey band delineates 95% confidence interval for test of equal univariate densities (n = 10,000 permutations). **e,** *In utero* electroporation of constitutively active PDGFRβ:D850V[23] (mouse E13.5-E15.5). Cortex was stained for SOX2; white arrowheads indicate co-labeling with electroporated GFP cells (quantified in **f**: at least n = 3 slices per embryo from 2 litters; n = 15 [control], n = 18 [PDGFRβ:D850V]; scale bar 50 μm). Note disrupted epithelial structure of VZ. Error bars = mean +/- s.e.m. Statistical significance for treatment was determined by ANOVA of multiple linear regression after controlling for individual (**b**) or litter (**d, f**) (n.s. $P > 0.05$, *$P \leq 0.05$, **$P \leq 0.01$, ***$P \leq 0.001$, ****$P \leq 0.0001$). **g,** Schematic summarizing experimental manipulations and results. LOF: loss-offunction, GOF: gain-of-function.